

This is an Open Access document downloaded from ORCA, Cardiff University's institutional repository: <https://orca.cardiff.ac.uk/id/eprint/132798/>

This is the author's version of a work that was submitted to / accepted for publication.

Citation for final published version:

Chen, Baile, Wan, Yating, Xie, Zhiyang, Huang, Jian, Zhang, Ningtao, Shang, Chen, Norman, Justin, Li, Qiang, Tong, Yeyu, Lau, Kei May, Gossard, Arthur C. and Bowers, John E. 2020. Low dark current high gain InAs quantum dot avalanche photodiodes monolithically grown on Si. *ACS Photonics* 7 (2), 528–533.
10.1021/acsp Photonics.9b01709

Publishers page: <http://dx.doi.org/10.1021/acsp Photonics.9b01709>

Please note:

Changes made as a result of publishing processes such as copy-editing, formatting and page numbers may not be reflected in this version. For the definitive version of this publication, please refer to the published source. You are advised to consult the publisher's version if you wish to cite this paper.

This version is being made available in accordance with publisher policies. See <http://orca.cf.ac.uk/policies.html> for usage policies. Copyright and moral rights for publications made available in ORCA are retained by the copyright holders.



Low dark current high gain InAs quantum dot avalanche photodetectors monolithically grown on Si

Baile Chen, YATING WAN, Zhiyang Xie, Jian Huang, Ningtao Zhang, Chen Shang, Justin Norman, Qiang Li, Yeyu Tong, Kei May Lau, Arthur C. Gossard, and John E. Bowers

ACS Photonics, **Just Accepted Manuscript** • DOI: 10.1021/acsp Photonics.9b01709 • Publication Date (Web): 08 Jan 2020

Downloaded from pubs.acs.org on January 8, 2020

Just Accepted

“Just Accepted” manuscripts have been peer-reviewed and accepted for publication. They are posted online prior to technical editing, formatting for publication and author proofing. The American Chemical Society provides “Just Accepted” as a service to the research community to expedite the dissemination of scientific material as soon as possible after acceptance. “Just Accepted” manuscripts appear in full in PDF format accompanied by an HTML abstract. “Just Accepted” manuscripts have been fully peer reviewed, but should not be considered the official version of record. They are citable by the Digital Object Identifier (DOI®). “Just Accepted” is an optional service offered to authors. Therefore, the “Just Accepted” Web site may not include all articles that will be published in the journal. After a manuscript is technically edited and formatted, it will be removed from the “Just Accepted” Web site and published as an ASAP article. Note that technical editing may introduce minor changes to the manuscript text and/or graphics which could affect content, and all legal disclaimers and ethical guidelines that apply to the journal pertain. ACS cannot be held responsible for errors or consequences arising from the use of information contained in these “Just Accepted” manuscripts.

Low dark current high gain InAs quantum dot avalanche photodetectors monolithically grown on Si

Baile Chen^{1,2, *†}, Yating Wan^{1, †}, Zhiyang Xie², Jian Huang², Ningtao Zhang², Chen Shang³, Justin Norman³, Qiang Li⁴, Yeyu Tong^{1,5}, Kei May Lau⁴, Arthur C. Gossard^{1,3,6}, John E. Bowers^{1,3,6}

*Corresponding Author: Baile Chen (chenbl@shanghaitech.edu.cn)

† These authors contributed equally to this work

¹Institute for Energy Efficiency, University of California Santa Barbara, Santa Barbara, CA, USA, 93106

²School of Information Science and Technology, ShanghaiTech University, Shanghai 201210, China

³Materials department, University of California Santa Barbara, Santa Barbara, CA, USA, 93106

⁴Department of Electronic and Computer Engineering, Hong Kong University of Science and Technology, Clear Water Bay, Hong Kong

⁵Department of Electronic Engineering, The Chinese University of Hong Kong, Hong Kong

⁶Department of Electrical and Computer Engineering, University of California Santa Barbara, Santa Barbara, CA, USA, 93106

Abstract: Avalanche photodetectors (APDs) on Si operating at optical communication wavelength band are crucial for Si-based transceiver application. In this paper, we report the first O-band InAs quantum dot (QD) waveguide avalanche photodetectors monolithically grown on Si with a low dark current of 0.1 nA at unit gain and a responsivity of 0.234 A/W at 1.310 μm at unit gain (-5V). In the linear gain mode, the APDs have a maximum gain of 198 and show a clear eye diagram up to 8 Gbit/s. These QD-based APDs enjoy the benefit of sharing the same epitaxial layers and processing flow as QD lasers, which could potentially facilitate the integration with laser sources on Si platform.

Keyword: quantum dots, silicon, avalanche photodetectors, gain, bandwidth

Self-assembled quantum-dot (QD) semiconductor nanostructures have attracted intense interest for optoelectronics devices applications due to their unique three-dimensional carrier confinement characteristic. Recently, O-band InAs QD lasers monolithically grown on Si substrate have been demonstrated with low threshold current, high temperature stability, and record-long device lifetime, which could potentially overcome the lack of laser source in Si photonics¹⁻⁴. Meanwhile, high performance optical amplifiers⁵, near infrared PIN waveguide PDs^{6,7}, mid-wavelength infrared QD photodetectors⁸⁻¹⁰ with similar QD structures on Si have been recently reported. The three-dimensional carrier confinement in the

1
2
3 QDs leads to ultra-low dark current density of $3.5 \times 10^{-7} \text{ A/cm}^2$ in QD PDs directly grown on (001) Si,
4
5 together with a decent responsivity around 0.2 A/W in the O-band ⁶.
6
7

8 Avalanche photodiodes (APDs) can achieve a high internal current gain by applying a high reverse bias
9
10 voltage due to the avalanche effect, which can significantly improve the signal to noise ratio ¹¹. Driven by
11
12 the increasing applications in optical communications, monolithic Si-Ge APDs have been demonstrated
13
14 with large gain-bandwidth products ¹². Recently, InAs QD APDs heterogeneously integrated on Si have
15
16 been reported with a low dark current of 0.01 nA and a high gain bandwidth product of 240 GHz ¹³. In this
17
18 work, we use an alternative approach through direct epitaxy for better economy of scale, better integration
19
20 with QD lasers, and demonstrate the first InAs QD APDs monolithically grown on (001) Si with a low dark
21
22 current of 0.1 nA in a $3 \times 50 \mu\text{m}^2$ device biased at -5V. The corresponding dark current density is as low
23
24 as $6.7 \times 10^{-5} \text{ A/cm}^2$, which is among the best reported values for any III-V PDs grown on a Si substrate at
25
26
27
28 the same reverse bias¹⁴⁻¹⁷. In addition, the PDs achieve a decent responsivity of 0.234 A/W at 1310 at unit
29
30 gain, limited by coupling into the photodetector waveguide. The dark current at 99% of breakdown voltage
31
32 is 1.3 nA, and an avalanche gain of up to 198 has been demonstrated. Due to RC and carrier trapping limits,
33
34 the APDs show 3-dB bandwidth of 2.26 GHz at -6 V. Temperature studies have been carried out to
35
36 understand the physics of the avalanche process in the devices. The limiting factors of the current device
37
38 have been analyzed and future improvements are discussed. Considering the high gain and low dark current
39
40 performance up to 323K (50 °C), these APDs hold great potential for applications in energy-efficient
41
42 interconnects within supercomputers and data centers.
43
44

45 **Device structure and Fabrication:**

46
47
48
49
50
51
52
53
54
55
56
57
58
59
60

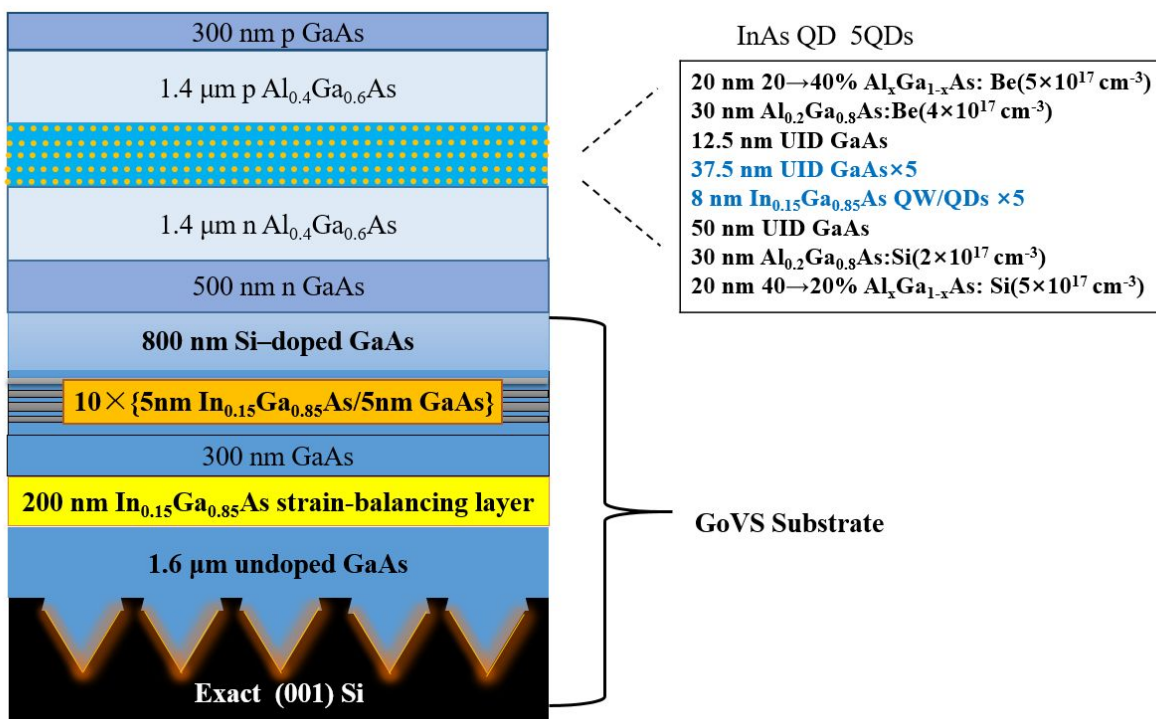


Figure 1. Schematic diagram of the InAs QDS APD grown on GoVS substrate.

The structure of the photodiode is shown in Fig. 1. The QD APD structure was grown on a GaAs-on-V-grooved-Si (GoVS) substrate, prepared by aspect ratio trapping (ART) in a metal-organic chemical vapor deposition (MOCVD) system^{18, 19}. The APD epitaxial structure was grown in a molecular beam epitaxy (MBE) system. The active region of the PD consists of five-stacked InAs dot-in-a-well (DWELL) structures, with a dot density of $6 \times 10^{10} \text{ cm}^{-2}$.

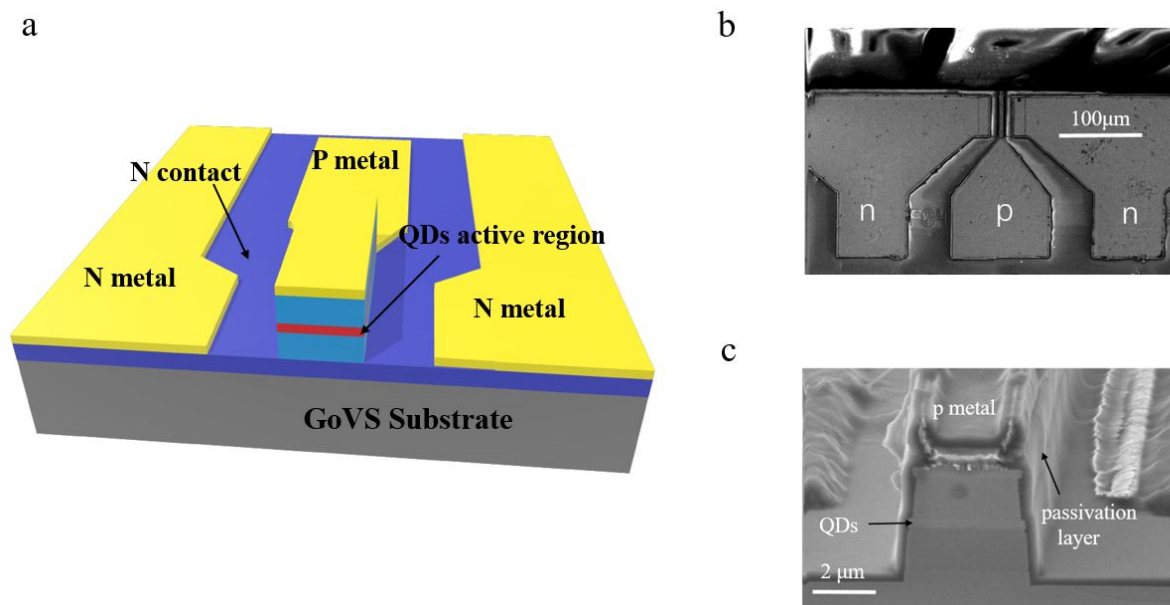


Figure 2. (a) Schematic diagram of the fabricated waveguide photodetector. (b) Top-view and (c) cross-sectional view of the fabricated device.

After the material growth, the epitaxial structure was processed into waveguide-shape APD devices with mesa widths ranging from 3 to 50 μm and mesa lengths of 50 μm by inductive coupled plasma (ICP) etching. After ICP etching, the sidewall was passivated with a 12-nm atomic-layer deposited (ALD) Al_2O_3 together with a 1- μm -thick SiO_2 layer to help suppress the surface leakage current. Pd/Ti/Pd/Au and Pd/Ge/Pd/Au were evaporated as metal contact stacks with a 150- μm pitch-size standard ground-signal-ground (GSG) pads. Finally, facets were cleaved with no additional anti-reflection coatings. The full device structure is schematically shown in Fig. 2(a). Top-view and cross-sectional view scanning electron microscope (SEM) images of a fabricated device are shown in Fig. 2(b) and Fig. 2(c), respectively.

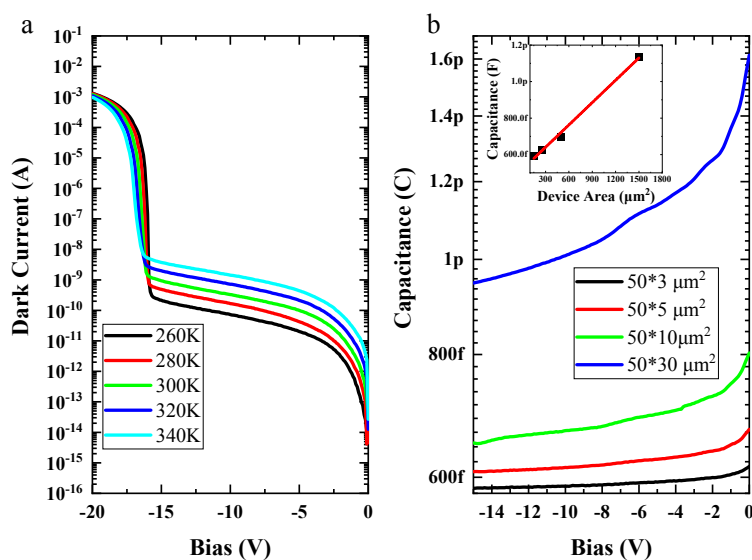


Figure 3. (a) Temperature dependent measurement of the Current-voltage characteristics of a $3 \times 50 \mu\text{m}^2$ device. (b) Capacitance voltage characteristics of devices with different size at room temperature. Inset: measured capacitance of a series of devices under -5V bias.

Measurement and analysis:

The dark current voltage (I-V) curves of a $3 \times 50 \mu\text{m}^2$ APD devices were measured from 260–340 K in a low temperature probe station and recorded by a semiconductor device analyzer (Keysight 1500), as shown in Fig. 3(a). The device shows a very low dark current of 0.1 nA at 300 K under a bias voltage of -5 V, which corresponds to a low dark current density of $6.6 \times 10^{-5} \text{A}/\text{cm}^2$. This can be attributed to the high crystal quality and surface passivation of the PD mesa. Moreover, the dark current at 300 K was measured to be 1.3 nA around -15.9 V, which is round 99% of the breakdown voltage (-16 V). It is also noted that the breakdown voltage of the APD increases as the temperature increases, which indicates the dominance of avalanche breakdown over tunneling in the APD structure. The capacitance voltage (C-V) characteristics of several different sizes of APD devices were also measured at room temperature as shown in Fig. 3(b), a parasitic capacitance of 517 fF was extracted based on the device area-capacitance curve in the inset of Fig. 3(b).

The gain versus bias voltage of the device at various temperatures were measured as shown in Fig. 4(a) with input wavelength of 1300nm. Here we take the unity gain bias of -5 V, to make sure the device is fully

depleted. The maximum gain value of 198 was obtained at 293K (20 °C), and drops to around 73 at 323K (50 °C). It's also noted that the dark current of the APD is only 33 nA while a maximum gain value of 198 is achieved at a reverse bias of -15.97 V at 293K (20 °C). This dark current value is more than two orders of magnitude lower than that of Si/Ge APDs²⁰, InGaAs/InAlAs APDs on Si¹⁵ and the recent InAs QD APDs heterogeneously integrated on Si¹³. The excess noise the APD is also measured by a noise figure meter as shown in the Fig. 4(b). The excess noise is high due to the mixed injection in the APD device and further optimization for minimizing the noise performance is necessary for future work.

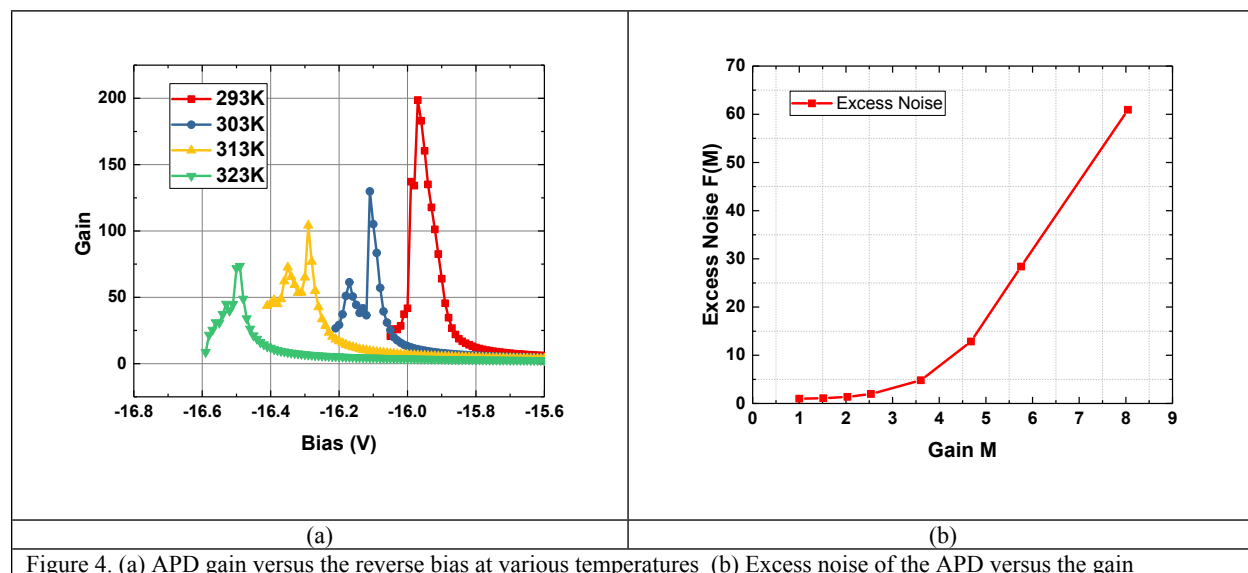


Figure 4. (a) APD gain versus the reverse bias at various temperatures (b) Excess noise of the APD versus the gain

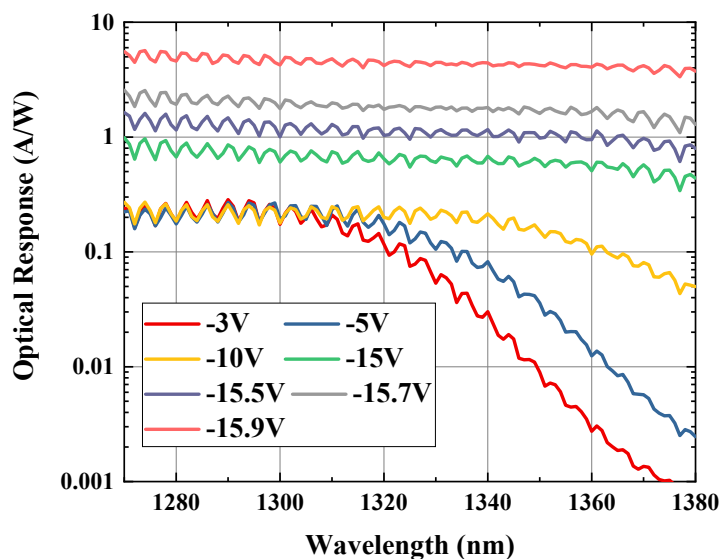
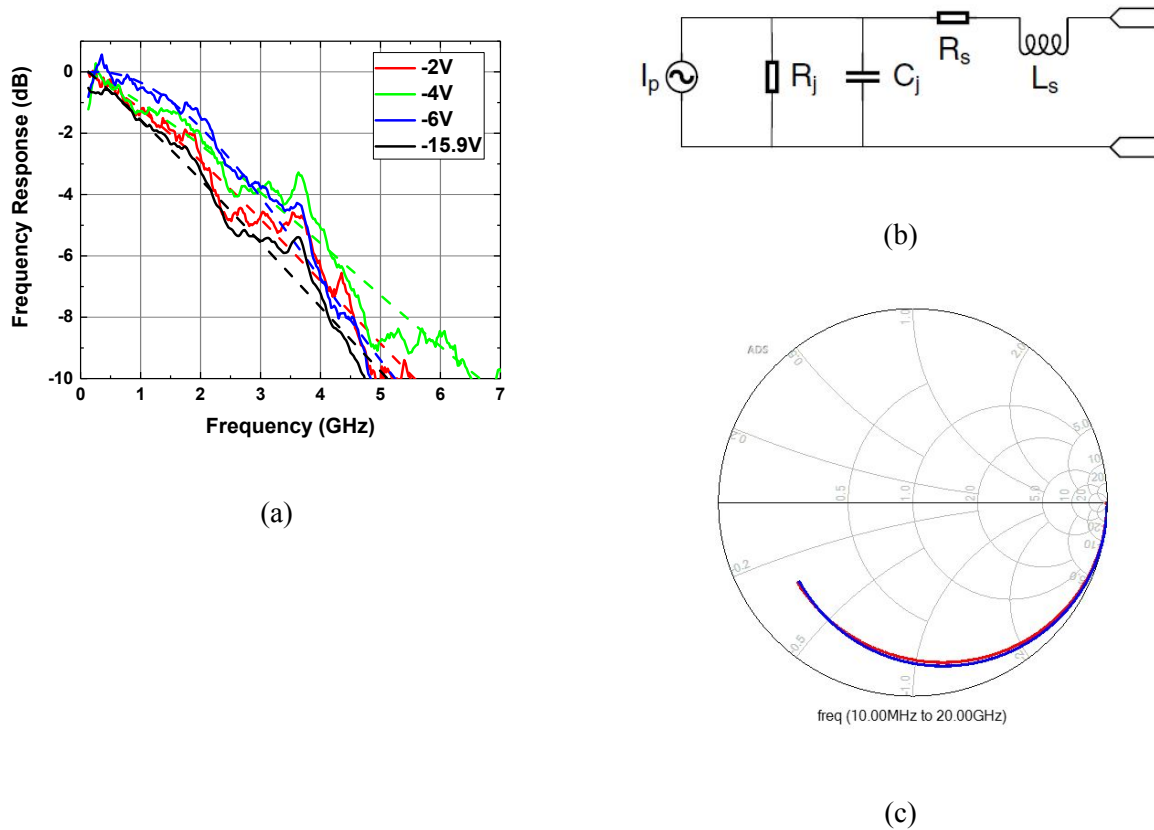


Figure 5. Wavelength dependence of APD responsivity at various biases.

Optical response of the APD was measured by coupling light with a lensed fiber from an O band tunable laser source to the cleaved facet of the PDs and adjusting the input polarization by a polarization controller. Fig. 5(a) shows wavelength dependence of responsivity for a $3 \times 50 \mu\text{m}^2$ device at different bias. The input power was fixed at -20 dbm so that the APD is not saturated during measurement at high gain condition. The coupling loss between the spherical-lensed fiber and the cleaved facet was estimated to be roughly 3 dB, which is estimated by comparing the measured power from an integrated sphere power meter and a fiber coupled power meter of a forward biased laser diode with the same epilayer structure and the same mesa width of the PD in this work. The oscillatory features shown in the responsivity plot is due to the Fabry-Perot resonance between the rear and the front facets, which has also shown up in other waveguide PD structures⁷. The responsivity of the device at -5 V is 0.234 A/W at 1310 nm and cuts off around 1360 nm, which corresponds to the bandgap of the InAs QD materials. The corresponding absorption coefficient at 1310nm is estimated to be 770 cm^{-1} , assuming a confinement factor of 6.5%. As the reverse bias increases, the cutoff wavelength red-shifts due to the quantum-confined Stark effect (QCSE), which shifts the electron states to lower energies and the hole states to higher energies, respectively, in the QD layers. At a reverse

1
2
3 bias of 15.9 V, the responsivity of the APD around 1310 nm increased to 4.8 A/W, due to the avalanche
4
5 gain of around 20 in the APD structure.
6
7
8
9
10
11
12
13
14
15
16
17
18
19
20



21
22
23
24
25
26
27
28
29
30
31
32
33
34
35
36
37
38
39
40
41
42
43
44
45
46
47 Figure 6 (a) Small-signal frequency responses of $3.0 \times 50 \mu\text{m}^2$ device for various bias voltages. (b) Equivalent circuit model
48 used for the fitting of the Impedance measurement. (c) Measured (red) and fitted (blue) curves of reflection S11 characteristics
49 from 10MHz to 20 GHz at -6V.
50

51
52 TABLE I. Fitting parameters in the circuit model Fig. 6(b).
53

R_s (Ω)	R_j ($M\Omega$)	C_j (fF)	L_s (fH)	f_{RC3dB} (GHz)
9.38	800	520	$1.08e-9$	5.16

1
2
3
4
5
6
7
8
9
10
11
12
13
14
15
16
17
18
19
20
21
22
23
24
25
26
27
28
29
30
31
32
33
34
35
36
37
38
39
40
41
42
43
44
45
46
47
48
49
50
51
52
53
54
55
56
57
58
59
60

1
2
3
4
5 The small-signal frequency response S_{21} was measured using a lightwave-component analyzer (LCA)
6 with a 1310 nm internal light source. The modulated light from LCA was input to the PD facet through a
7 lensed fiber. S_{21} characteristics of a $3 \times 50 \mu\text{m}^2$ device biased at various voltages is presented in Fig. 6(a).
8 As shown in Fig. 6(a), the 3dB bandwidth increases slightly as the reverse bias increases from -2V to -6V,
9 which is due to the reduction of both carrier transport time and carrier emission time out of quantum dots
10 as the electrical field in the absorption region increases. The 3-dB bandwidth of the device is 2.26 GHz
11 and 2.06 GHz at the bias of -6 V and -15.9V, respectively. The bandwidth reduction at -15.9V is due to the
12 avalanche built-up time. To assess the bandwidth limiting factors, S_{11} characteristics were measured and
13 the parameters were fitted with an equivalent circuit model (Fig. 6(b).), as shown in Fig. 6(c) ^{21, 22}. The
14 circuit parameters were de-embedded from the S_{11} characteristics, giving rise to a calculated RC-limited
15 bandwidth of 5.16 GHz with the corresponding fitting parameters shown in Table I. This RC limited
16 bandwidth is slightly larger to the measured bandwidth value, it is expected that the device performance
17 may be limited by both RC and transit time. As one of the future works, semi-insulator Si substrate or thick
18 benzocyclobutene (BCB) layer or SU8 layer can be used for material growth and device fabrication to
19 minimize the parasitic capacitance in the device, which could potentially improve the RC limited
20 performance^{23,24}.

21
22
23
24
25
26
27
28
29
30
31
32
33
34
35
36
37
38
39
40 Fig. 7 shows the eye diagram of a $3.0 \times 50 \mu\text{m}^2$ avalanche photodiode biased at -15.9 V and operating
41 at a 2.5 Gbit/s, 5 Gbit/s, and 8 Gbit/s data rate. $2^{31}-1$ pseudo-random binary sequence (PRBS) sequences
42 were generated as the data source to drive an O band lithium-niobate (LN) modulator, which modulates the
43 1.31 μm optical signal coming from an external tunable laser. The modulated light signal was controlled to
44 be TE light by a polarization controller and was used as an input to the device through a spherical lensed
45 fiber with an output input power of ~ 3 dBm. Clear eye opening up to a data-rate of 8 Gbit/s is demonstrated,
46 which indicates that these APDs can be used in an O-band optical communications system. The bit error
47 rate (BER) test at different bias points was conducted using an Anritsu Bit Error Rate Tester at 2.5 Gb/s at
48
49
50
51
52
53
54
55
56
57
58
59
60

room temperature, as shown Fig. 8. Photodiodes operated at high gain bias point of -15.9 V exhibit a significantly improved bit error rate as compared to the lower bias point with the same input optical power.

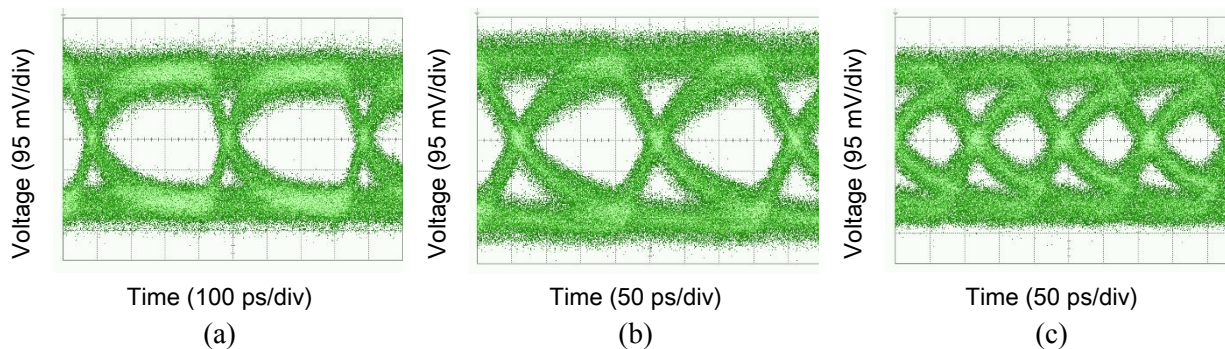


Figure 7. Measured eye diagrams at a bias voltage of -15.9 V for data-rate of 2.5 Gbit/s, 5 Gbit/s and 8 Gbit/s.

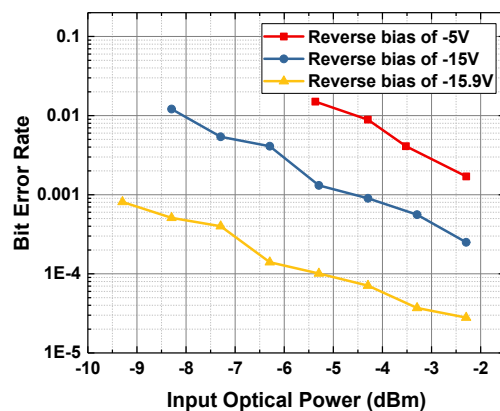


Figure 8. BER versus input optical power of a $3\ \mu\text{m} \times 50\ \mu\text{m}$ PD with different reverse bias points at 1310 nm

It's also noted that the APD structure demonstrated in this work is based on the PIN QD structures operated under high reverse bias. The QDs layer here acts as both absorption region and multiplication region, which could cause high excess noise in the APD considering the mixed carrier injection¹¹. The expected high excess noise of the APD also limited the signal to noise ratio when operated at high gain bias

point. One way to overcome this drawback is to incorporate the separated absorption, charge and multiplication avalanche photodiode (SACM-APD) for low noise and high speed applications^{25,26}.

Conclusions:

In summary, we reported the first InAs QD APDs grown on (001) Si using the same epitaxial layers and fabrication process for a QD laser. A low dark current density of $6.7 \times 10^{-5} \text{ A/cm}^2$ has been achieved, which is more than 2 orders of magnitude lower than Ge/Si APDs. A high avalanche gain up to 198 was demonstrated and the limiting factors of the 3-dB bandwidth of these QD APDs have been investigated. Open eye diagrams were measured up to 8 Gbit/s, which show potential for the O-band optical communications system.

Acknowledgements

This work was funded in part by the National Key Research and Development Program of China (No. 2018YFB2201000), in part by the Shanghai Sailing Program (17YF1429300), in part by ShanghaiTech University startup funding (F-0203-16-002), and in part by the Advanced Research Projects Agency-Energy (ARPA-E), U.S. Department of Energy, under Award Number DE-AR0001042.

References

1. Chen, S.; Liao, M.; Tang, M.; Wu, J.; Martin, M.; Baron, T.; Seeds, A.; Liu, H., Electrically pumped continuous-wave 1.3 μm InAs/GaAs quantum dot lasers monolithically grown on on-axis Si (001) substrates. *Optics express* **2017**, *25* (5), 4632-4639.
2. Chen, S.; Li, W.; Wu, J.; Jiang, Q.; Tang, M.; Shutts, S.; Elliott, S. N.; Sobiesierski, A.; Seeds, A. J.; Ross, I., Electrically pumped continuous-wave III-V quantum dot lasers on silicon. *Nature Photonics* **2016**, *10* (5), 307.
3. Wan, Y.; Zhang, S.; Norman, J. C.; Kennedy, M.; He, W.; Liu, S.; Xiang, C.; Shang, C.; He, J.-J.; Gossard, A. C., Tunable quantum dot lasers grown directly on silicon. *Optica* **2019**, *6* (11), 1394-1400.
4. Norman, J. C.; Jung, D.; Wan, Y.; Bowers, J. E., Perspective: The future of quantum dot photonic integrated circuits. *APL Photonics* **2018**, *3* (3), 030901.
5. Liu, S.; Norman, J.; Dumont, M.; Jung, D.; Torres, A.; Gossard, A. C.; Bowers, J. E.; Liu, S.; Torres, A.; Gossard, A., High-Performance O-Band Quantum-Dot Semiconductor Optical Amplifiers Directly Grown on a CMOS Compatible Silicon Substrate. *ACS Photonics* **2019**, *6* (10), 2523-2529.
6. Huang, J.; Wan, Y.; Jung, D.; Norman, J.; Shang, C.; Li, Q.; Lau, K. M.; Gossard, A. C.; Bowers, J. E.; Chen, B., Defect Characterization of InAs/InGaAs Quantum Dot p-i-n Photodetector Grown on GaAs-on-V-Grooved-Si Substrate. *ACS Photonics* **2019**, *6* (5), 1100-1105.

7. Wan, Y.; Zhang, Z.; Chao, R.; Norman, J.; Jung, D.; Shang, C.; Li, Q.; Kennedy, M.; Liang, D.; Zhang, C., Monolithically integrated InAs/InGaAs quantum dot photodetectors on silicon substrates. *Optics express* **2017**, *25* (22), 27715-27723.
8. Chen, W.; Deng, Z.; Guo, D.; Chen, Y.; Mazur, Y.; Maidaniuk, Y.; Benamara, M.; Salamo, G. J.; Liu, H.; Wu, J., Demonstration of InAs/InGaAs/GaAs Quantum Dots-in-a-well Mid-wave Infrared Photodetectors Grown on Silicon Substrate. *Journal of Lightwave Technology* **2018**, *36* (13), 2572 - 2581.
9. Huang, J.; Guo, D.; Deng, Z.; Chen, W.; Liu, H.; Wu, J.; Chen, B., Midwave Infrared Quantum Dot Quantum Cascade Photodetector Monolithically Grown on Silicon Substrate. *Journal of Lightwave Technology* **2018**, *36* (18), 4033-4038.
10. Wu, J.; Jiang, Q.; Chen, S.; Tang, M.; Mazur, Y. I.; Maidaniuk, Y.; Benamara, M.; Semtsiv, M. P.; Masselink, W. T.; Sablon, K. A., Monolithically integrated InAs/GaAs quantum dot mid-infrared photodetectors on silicon substrates. *ACS Photonics* **2016**, *3* (5), 749-753.
11. Campbell, J. C., Recent Advances in Avalanche Photodiodes. *Journal of Lightwave Technology* **2016**, *34* (2), 278-285.
12. Kang, Y.; Liu, H.-D.; Morse, M.; Paniccia, M. J.; Zadka, M.; Litski, S.; Sarid, G.; Pauchard, A.; Kuo, Y.-H.; Chen, H.-W., Monolithic germanium/silicon avalanche photodiodes with 340 GHz gain–bandwidth product. *Nature photonics* **2009**, *3* (1), 59.
13. Tossoun, B.; Kurczveil, G.; Zhang, C.; Descos, A.; Huang, Z.; Beling, A.; Campbell, J. C.; Liang, D.; Beausoleil, R. G., Indium arsenide quantum dot waveguide photodiodes heterogeneously integrated on silicon. *Optica* **2019**, *6* (10), 1277-1281.
14. Geng, Y.; Feng, S.; Poon, A. W.; Lau, K. M., High-speed InGaAs photodetectors by selective-area MOCVD toward optoelectronic integrated circuits. *IEEE Journal of Selected Topics in Quantum Electronics* **2014**, *20* (6), 36-42.
15. Yuan, Y.; Jung, D.; Sun, K.; Zheng, J.; Jones, A. H.; Bowers, J. E.; Campbell, J. C., III-V on silicon avalanche photodiodes by heteroepitaxy. *Optics letters* **2019**, *44* (14), 3538-3541.
16. Inoue, D.; Wan, Y.; Jung, D.; Norman, J.; Shang, C.; Nishiyama, N.; Arai, S.; Gossard, A.; Bowers, J., Low-dark current 10 Gbit/s operation of InAs/InGaAs quantum dot pin photodiode grown on on-axis (001) GaP/Si. *Applied Physics Letters* **2018**, *113* (9), 093506.
17. Sandall, I.; Ng, J. S.; David, J. P.; Tan, C. H.; Wang, T.; Liu, H., 1300 nm wavelength InAs quantum dot photodetector grown on silicon. *Optics express* **2012**, *20* (10), 10446-10452.
18. Shang, C.; Wan, Y.; Norman, J. C.; Collins, N.; MacFarlane, I.; Dumont, M.; Liu, S.; Li, Q.; Lau, K. M.; Gossard, A. C., Low-Threshold Epitaxially Grown 1.3- μm InAs Quantum Dot Lasers on Patterned (001) Si. *IEEE Journal of Selected Topics in Quantum Electronics* **2019**, *25* (6), 1-7.
19. Li, Q.; Wan, Y.; Liu, A. Y.; Gossard, A. C.; Bowers, J. E.; Hu, E. L.; Lau, K. M., 1.3- μm InAs quantum-dot micro-disk lasers on V-groove patterned and unpatterned (001) silicon. *Optics express* **2016**, *24* (18), 21038-21045.
20. Huang, Z.; Li, C.; Liang, D.; Yu, K.; Santori, C.; Fiorentino, M.; Sorin, W.; Palermo, S.; Beausoleil, R. G., 25 Gbps low-voltage waveguide Si–Ge avalanche photodiode. *Optica* **2016**, *3* (8), 793-798.
21. Chen, Y.; Xie, Z.; Huang, J.; Deng, Z.; Chen, B., High-speed uni-traveling carrier photodiode for 2 μm wavelength application. *Optica* **2019**, *6* (7), 884-889.
22. Xie, Z.; Chen, Y.; Zhang, N.; Chen, B., InGaAsP/InP Uni-Traveling-Carrier Photodiode at 1064-nm Wavelength. *IEEE Photon. Technol. Lett.* **2019**, *31* (16), 1331-1334.
23. Chen, Y.; Chai, X.; Xie, Z.; Deng, Z.; Zhang, N.; Zhou, Y.; Xu, Z.; Chen, J.; Chen, B., High-Speed Mid-Infrared Interband Cascade Photodetector Based on InAs/GaAsSb Type-II Superlattice. *Journal of Lightwave Technology* **2019**, DOI: 10.1109/JLT.2019.2950607.

- 1
2
3 24. Chen, Y.; Zhao, X.; Huang, J.; Deng, Z.; Cao, C.; Gong, Q.; Chen, B., Dynamic model and
4 bandwidth characterization of InGaAs/GaAsSb type-II quantum wells PIN photodiodes. *Optics express*
5 **2018**, *26* (26), 35034-35045.
- 6 25. Duan, N.; Wang, S.; Ma, F.; Li, N.; Campbell, J. C.; Wang, C.; Coldren, L. A., High-speed and
7 low-noise SACM avalanche photodiodes with an impact-ionization-engineered multiplication region.
8 *IEEE Photonics Technology Letters* **2005**, *17* (8), 1719-1721.
- 9 26. Ma, Y. J.; Zhang, Y. G.; Gu, Y.; Chen, X. Y.; Wang, P.; Juang, B. C.; Farrell, A.; Liang, B. L.;
10 Huffaker, D. L.; Shi, Y. H., Enhanced Carrier Multiplication in InAs Quantum Dots for Bulk Avalanche
11 Photodetector Applications. *Advanced Optical Materials* **2017**, *5* (9), 1601023.
- 12
13
14
15
16
17
18
19
20
21

